pH-Dependent Transfer Hydrogenation, Reductive Amination, and Dehalogenation of Water-Soluble Carbonyl Compounds and Alkyl Halides Promoted by Cp*Ir Complexes

Seiji Ogo,*[,†,‡] Nobuyuki Makihara,[‡] Yuichi Kaneko,[§] and Yoshihito Watanabe*[,†,‡,∥]

Institute for Molecular Science, Myodaiji, Okazaki 444-8585, Japan, Department of Structural Molecular Science, The Graduate University for Advanced Studies, Myodaiji, Okazaki 444-8585, Japan, Department of Chemistry, Faculty of Science, Kochi University, Akebono-cho, Kochi 780-8520, Japan, and Center for Integrative Bioscience, Myodaiji, Okazaki 444-8585, Japan

Received June 15, 2001

Downloaded by CARLI CONSORTIUM on June 29, 2009
Published on September 27, 2001 on http://pubs.acs.org | doi: 10.1021/om010523v

This paper reports pH-dependent transfer hydrogenation, reductive amination, and dehalogenation of water-soluble substrates with the organometallic aqua complexes $[Cp^*Ir^{III}(H_2O)_3]^{2+}$ (**1**, Cp* = η^5-pentamethylcyclopentadienyl), $[(Cp\wedge py)Ir^{III}(H_2O)_2]^{2+}$ (**2**, Cp∧py = η^5-(tetramethylcyclopentadienyl)methylpyridine), and $[Cp^*Ir^{III}(bpy)(H_2O)]^{2+}$ (**3**, bpy = 2,2′-bipyridine) as catalyst precursors and the formate ions HCOONa and $HCOONH_4$ as hydrogen donors. Because of the difference in the electron-donating ability of the Cp*, Cp∧py, and bpy ligands, the Lewis acidity of the iridium ions of **1**−**3** are ordered in strength as follows: **1** > **2** > **3**. Complexes **1**−**3** are reversibly deprotonated to form the catalytically inactive hydroxo complexes $[(Cp^*Ir^{III})_2(\mu\text{-}OH)_3]^+$ (**5**), $[\{(Cp\wedge py)Ir^{III}\}_2(\mu\text{-}OH)_2]^{2+}$ (**6**), and $[Cp^*Ir^{III}(bpy)(OH)]^+$ (**7**) around pH 2.8, 4.5, and 6.6, respectively. The deprotonation behavior of **1**−**3** indicates that the more Lewis acidic iridium ions would lower the pK_a values of the coordinated H_2O ligands. As a function of pH, the catalyst precursors **1** and **3** react with the formate ions to form the hydride complexes $[(Cp^*Ir^{III})_2(\mu\text{-}H)(\mu\text{-}OH)(\mu\text{-}HCOO)]^+$ (**8**) and $[Cp^*Ir^{III}(bpy)(H)]^+$ (**9**), respectively, which act as active catalysts in these catalytic reductions. A similar hydride complex would be formed from the reaction of **2** with the formate ions, though we have no definite structural information on the hydride complex. The structures of $\mathbf{3}(OTf)_2\cdot H_2O$ (OTf = $CF_3SO_3^-$), $[(Cp\wedge py)Ir^{III}Cl_2]$ (**4**), $\mathbf{6}(OTf)_2$, $\mathbf{7}(OTf)\cdot 2H_2O$, and $\mathbf{8}(PF_6)$ were unequivocally determined by X-ray analysis.

Introduction

Development of water-soluble organometallic catalysts is a worthy endeavor because of potential advantages such as reaction-specific pH selectivity, introduction of new biphasic processes, and alleviation of environmental problems associated with the use of organic solvents.[1] Although the majority of these studies have been carried out with water-soluble organometallic complexes containing water-soluble phosphine ligands,[2] few have utilized organometallic complexes containing water molecules as ligands (i.e. organometallic aqua complexes).[3] These organometallic aqua complexes are promising new pH-selective catalysts, since their structures drastically change as a function of pH due to deprotonation of the H_2O ligands.

Recently, we reported a pH-dependent transfer hydrogenation of water-soluble carbonyl compounds with the aqua complex $[Cp^*Ir^{III}(H_2O)_3]^{2+}$ (**1**, Cp* = η^5-pentamethylcyclopentadienyl) as a catalyst precursor and HCOONa as a hydrogen donor.[3a] We have extended our study with **1** to that with $[(Cp\wedge py)Ir^{III}(H_2O)_2]^{2+}$ (**2**, Cp∧py = η^5-(tetramethylcyclopentadienyl)methylpyridine) and $[Cp^*Ir^{III}(bpy)(H_2O)]^{2+}$ (**3**, bpy = 2,2′-

* To whom all correspondence should be addressed.
† Institute for Molecular Science.
‡ The Graduate University for Advanced Studies.
§ Kochi University.
∥ Center for Integrative Bioscience.

(1) (a) Cornils, B. *J. Mol. Catal. A* **1999**, *143*, 1−20. (b) Nomura, K. *J. Mol. Catal. A* **1998**, *130*, 1−28. (c) Cornils, B.; Herrmann, W. A. In *Aqueous-Phase Organometallic Catalysis*; Wiley-VCH: Weinheim, Germany, 1998; p 615. (d) Joó, F.; Kovács, J.; Kathó, Á.; Bényei, A. C.; Decuir, T.; Darensbourg, D. J. *Inorg. Synth.* **1998**, *32*, 1−45. (e) Augé, J.; Beletskaya, I. P.; Cheprakov, A. V.; Fringuelli, F.; Gajewski, J. J.; Garner, P. P.; Grieco, P. A.; Kobayashi, S.; Lubineau, A.; Parker, D. T.; Piermatti, O.; Pizzo, F.; Queneau, Y. In *Organic Synthesis in Water*; Grieco, P. A., Ed.; Thomson Science: London, 1998; p 310. (f) Li, C.-J.; Chan, T.-H. In *Organic Reactions in Aqueous Media*; Wiley: New York, 1997; p 199. (g) Joó, F.; Kathó, Á. *J. Mol. Catal. A* **1997**, *116*, 3−26. (h) Horváth, I. T.; Joó, F. In *Aqueous Organometallic Chemistry and Catalysis*; Kluwer Academic: Dordrecht, The Netherlands, 1995; p 317. (i) Roundhill, D. M. *Adv. Organomet. Chem.* **1995**, *38*, 155−188. (j) Chaloner, P. A.; Esteruelas, M. A.; Joó, F.; Oro, L. A. In *Homogeneous Hydrogenation*; Kluwer Academic: Dordrecht, The Netherlands, 1994; p 287. (k) Herrmann, W. A.; Kohlpaintner, C. W. *Angew. Chem., Int. Ed. Engl.* **1993**, *32*, 1524−1544.

(2) (a) Joó, F.; Kovács, J.; Bényei, A. C.; Nádasdi, L.; Laurenczy, G. *Chem. Eur. J.* **2001**, *7*, 193−199. (b) Kovács, J.; Todd, T. D.; Reibenspies, J. H.; Joó, F.; Darensbourg, D. J. *Organometallics* **2000**, *19*, 3963−3969. (c) Tin, K.-C.; Wong, N.-B.; Li. R−X.; Li, Y.-Z.; Hu, J.-Y.; Li, X.-J. *J. Mol. Catal. A* **1999**, *137*, 121−125. (d) Joó, F.; Kovács, J.; Bényei, A. C.; Kathó, Á. *Angew. Chem., Int. Ed. Engl.* **1998**, *37*, 969−970. (e) Joó, F.; Nádasdi, L.; Bényei, A. C.; Darensbourg, D. J. *J. Organomet. Chem.* **1996**, *512*, 45−50.

10.1021/om010523v CCC: $20.00 © 2001 American Chemical Society
Publication on Web 09/27/2001

Scheme 1

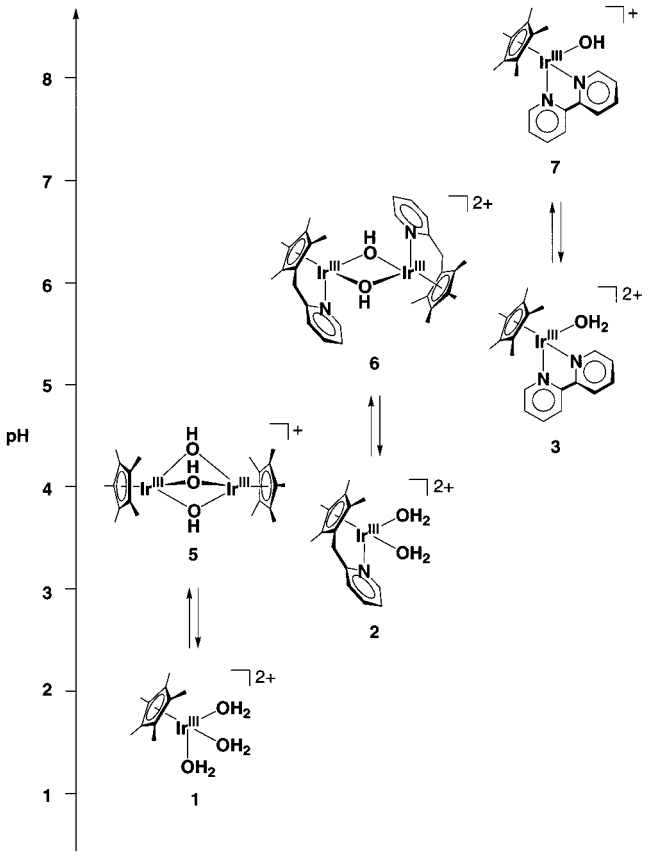

bipyridine), since we expect that the ligation of pyridine and bipyridine in **1** could change its catalytic activity due to the change of the Lewis acidity of the iridium ion. Herein, we report preliminary findings of pH-dependent transfer hydrogenation,[4] reductive amination,[5] and dehalogenation[6] of water-soluble carbonyl compounds and alkyl halides with **1**−**3** as catalyst precursors and HCOONa and $HCOONH_4$ as hydrogen donors. The pH dependence in these reactions is discussed on the basis of (i) deprotonation processes of the catalyst precursors (Scheme 1), (ii) pH-dependent behavior of the hydrogen donors, and (iii) pH-dependent formation of the active catalysts.

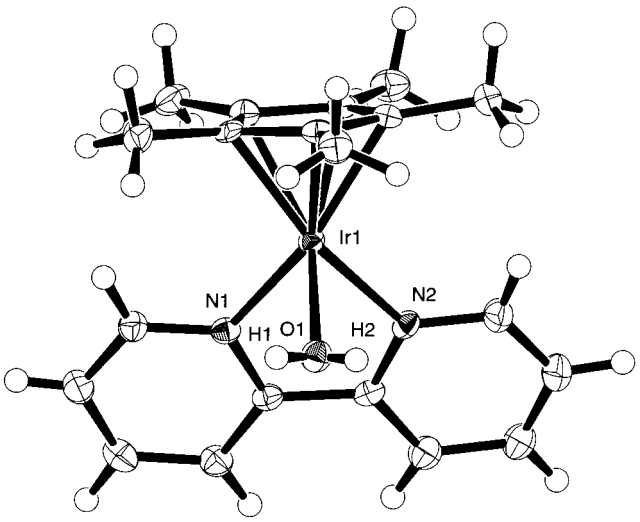

Figure 1. ORTEP drawing of **3**. The anions (OTf) are omitted for clarity. Selected bond lengths (Å) and angles (deg): Ir1−O1 = 2.154(2), Ir1−N1 = 2.084(2), Ir1−N2 = 2.103(2); O1−Ir1−N1 = 81.16(9), O1−Ir1−N2 = 80.59(9), N1−Ir1−N2 = 77. 01(9).

Results and Discussion

The New Ligand H(Cp∧py). The new ligand H(Cp∧py) was designed to prepare an Ir^{III} center having the formation of $Ir^{III}-(\eta^5\text{-}C_5Me_4)$ and $Ir^{III}-(NC_5H_4)$ bonds with potentially two vacant coordination sites on the metal center. In aqueous media, these vacant coordination sites should be occupied by weakly bound H_2O molecules that can be readily displaced by exogenous substrates. H(Cp∧py) was synthesized from the reaction of 2-picoline, lithium diisopropylamide (LDA), 2,3,4,5-tetramethyl-2-cyclopentenone, and *p*-toluenesulfonic acid (see Experimental Section).

Catalyst Precursors. The aqua complexes **1** and **3** were prepared by the method described in the previous paper.[3a,b] We have determined the crystal structure of **3**$(OTf)_2 \cdot H_2O$ (OTf = $CF_3SO_3^-$) by X-ray analysis.[7,8] All hydrogen atoms, which were located at the positions generated by Fourier-difference syntheses, were included in the least-squares calculation of **3**. As shown in Figure 1, complex **3** adopts distorted-octahedral

Downloaded by CARLI CONSORTIUM on June 29, 2009
Published on September 27, 2001 on http://pubs.acs.org | doi: 10.1021/om010523v

(3) (a) Ogo, S.; Makihara, N.; Watanabe, Y. *Organometallics* **1999**, *18*, 5470−5474. (b) Dadci, L.; Elias, H.; Frey, U.; Hörnig, A.; Koelle, U.; Merbach, A. E.; Paulus, H.; Schneider, J. S. *Inorg. Chem.* **1995**, *34*, 306−315. (c) Makihara, N.; Ogo, S.; Watanabe, Y. *Organometallics* **2001**, *20*, 497−500. (d) Poth, T.; Paulus, H.; Elias, H.; Ducker-Benfer, C.; Eldik, R. V. *Eur. J. Inorg. Chem.* **2001**, 1361−1369. (e) Cayemittes, S.; Poth, T.; Fernandez, M. J.; Lye, P. G.; Becker, M.; Elias, H.; Merbach, A. E. *Inorg. Chem.* **1999**, *38*, 4309−4316. (f) Faure, M.; Vallina, A. T.; Stoeckli-Evans, H.; Süss-Fink, G. *J. Organomet. Chem.* **2001**, *621*, 103−108. (g) Cayemittes, S.; Poth, T.; Fernandez, M. J.; Lye, P. G.; Becker, M.; Elias, H.; Merbach, A. E. *Inorg. Chem.* **1999**, *38*, 4309−4316. (h) Lo, H. C.; Buriez, O.; Kerr, J. B.; Fish, R. H. *Angew. Chem., Int. Ed.* **1999**, *38*, 1429−1432. (i) Mahon, M. F.; Whittlesey, M. K.; Wood, P. T. *Organometallics* **1999**, *18*, 4068−4074. (j) Fidalgo, E. G.; Plasseraud, L.; Süss-Fink, G. *J. Mol. Catal. A* **1998**, *132*, 5−12. (k) Egli, A.; Hegetschweiler, K.; Alberto, R.; Abram, U.; Schibli, R.; Hedinger, R.; Gramlich, V.; Kissner, R.; Schubiger, P. A. *Organometallics* **1997**, *16*, 1833−1840. (l) Richens, D. T. In *The Chemistry of Aqua Ions*; Wiley: West Sussex, U.K., 1997; p 592. (m) Ogo, S.; Chen, H.; Olmstead, M. M.; Fish, R. H. *Organometallics* **1996**, *15*, 2009−2013. (n) Kölle, U.; Görissen, R.; Wagner, T. *Chem. Ber.* **1995**, *128*, 911−917. (o) Eisen, M. S.; Haskel, A.; Chen, H.; Olmstead, M. M.; Smith, D. P.; Maestre, M. F.; Fish, R. H. *Organometallics* **1995**, *14*, 2806−2812. (p) Meister, G.; Rheinwald, G.; Stoeckli-Evans, H.; Süss-Fink, G. *J. Chem. Soc., Dalton Trans.* **1994**, 3215−3223. (q) Koelle, U. *Coord. Chem. Rev.* **1994**, *135/136*, 623−650.

(4) (a) Darensbourg, D. J.; Stafford, N. W.; Joó, F.; Reibenspies, J. H. *J. Organomet. Chem.* **1995**, *488*, 99−108. (b) Darensbourg, D. J.; Joó, F.; Kannisto, M.; Kathó, A.; Reibenspies, J. H.; Daigle, D. J. *Inorg. Chem.* **1994**, *33*, 200−208. (c) Darensbourg, D. J.; Joó, F.; Kannisto, M.; Kathó, A.; Reibenspies, J. H. *Organometallics* **1992**, *11*, 1990−1993. (d) Bényei, A.; Joó, F. *J. Mol. Catal.* **1990**, *58*, 151−163.

(5) (a) Chandrasekhar, S.; Reddy, C. R.; Ahmed, M. *Synlett* **2000**, *11*, 1655−1657. (b) Zimmermann, B.; Herwig, J.; Beller, M. *Angew. Chem., Int. Ed.* **1999**, *38*, 2372−2375. (c) Schaffrath, H.; Keim, W. *J. Mol. Catal. A* **1999**, *140*, 107−113.

(6) (a) Bényei, A. C.; Lehel, S.; Joó, F. *J. Mol. Catal. A* **1997**, *116*, 349−354. (b) Rajagopal, S.; Spatola, A. F. *J. Org. Chem.* **1995**, *60*, 1347−1355. (c) Marques, C. A.; Selva, M.; Tundo, P. *J. Org. Chem.* **1995**, *60*, 2430−2435. (d) Ram, S.; Ehrenkaufer, R. E. *Synthesis* **1988**, 91−95.

(7) Crystallographic data for **3**$(OTf)_2 \cdot H_2O$, **4**, **6**$(OTf)_2$, **7**$(OTf) \cdot 2H_2O$, and **8**(PF_6) have been deposited with the Cambridge Crystallographic Data Center as Supplementary Publication Nos. CCDC-165018, CCDC-165019, CCDC-165020, CCDC-165021, and CCDC-165022, respectively. Copies of the data can be obtained free of charge on application to the CCDC, 12 Union Road, Cambridge CB21EZ, U.K. (fax, (+44)-1223-336-033; e-mail, deposit@ccdc.cam.ac.uk).

(8) Crystal data for **3**$(OTf)_2 \cdot H_2O$: $C_{22}H_{27}F_6IrN_2O_8S_2$, MW 817.79, monoclinic, space group $P2_1/c$ (No. 14), a = 12.4763(8) Å, b = 15.673-(2) Å, c = 14.2297(2) Å, β = 97.8997(5)°, V = 2756.0(3) Å^3, Z = 4, D_c = 1.971 g cm^{-3}, μ(Mo Kα) = 50.99 cm^{-1}, R = 0.035, and R_w = 0.051.

Downloaded by CARLI CONSORTIUM on June 29, 2009
Published on September 27, 2001 on http://pubs.acs.org | doi: 10.1021/om010523v

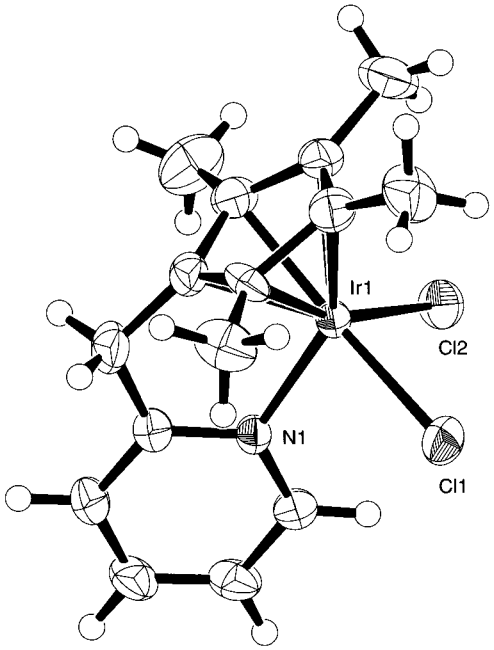

Figure 2. ORTEP drawing of **4**. Selected bond lengths (Å) and angles (deg): Ir1−Cl1 = 2.410(2), Ir1−Cl2 = 2.403-(2), Ir1−N1 = 2.100(5); Cl1−Ir1−Cl2 = 91.78(6), Cl1−Ir1−N1 = 89.8(1), Cl2−Ir1−N1 = 89.9(1).

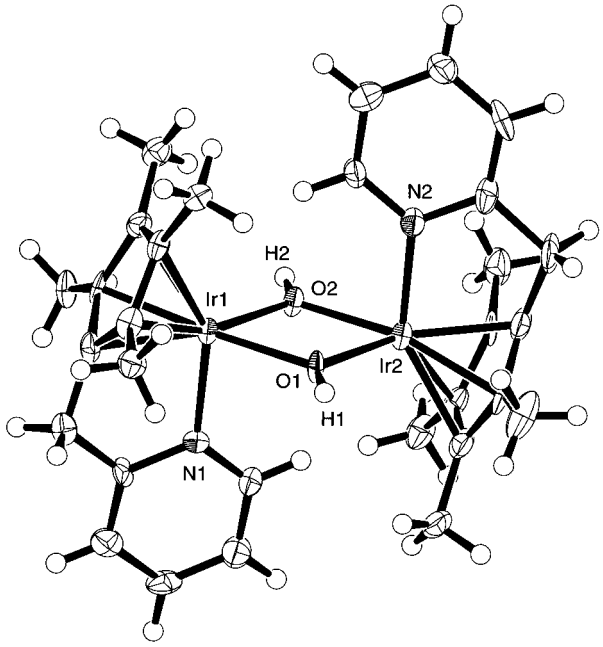

Figure 3. ORTEP drawing of **6**. The anions (OTf) are omitted for clarity. Selected bond lengths (Å) and angles (deg): Ir1−O1 = 2.111(6), Ir1−O2 = 2.117(7), Ir1−N1 = 2.093(7), Ir2−O1 = 2.119(6), Ir2−O2 = 2.106(7), Ir2−N2 = 2.105(8); O1−Ir1−O2 = 71.6(2), O1−Ir2−O2 = 71.7(2), Ir1−O1−Ir2 = 108.2(3), Ir1−O2−Ir2 = 108.4(3), O1−Ir1−N1 = 87.1(3), O2−Ir1−N1 = 92.3(3), O1−Ir2−N2 = 94.7-(3), O2−Ir2−N2 = 86.6(3).

coordination which is surrounded by one Cp*, one bpy, and one H_2O ligand. The torsion angle between the least-squares plane of Cp* and that of bpy is 60.9(1)°. The aqua complex **2** was synthesized from the reaction of $AgBF_4$ with [(Cp∧py)$Ir^{III}Cl_2$] (**4**) which was prepared by the reaction of $IrCl_3 \cdot 3H_2O$ with H(Cp∧py). The structure of **4** was determined by X-ray analysis (Figure 2).[7,9] Complex **4** has a distorted-octahedral coordination with two perpendicular planes (the torsion angle between the least-squares plane of η^5-C_5Me_4 and that of C_5H_4N = 85.3(3)°) as a result of the formation of the expected Ir^{III}−(η^5-C_5Me_4) and Ir^{III}−(NC_5H_4) bonds.

Deprotonation Processes of the Catalyst Precursors. ^{1}H NMR experiments show that, around pH 2.8 (pD 3.2),[10] the catalyst precursor **1** (Cp* at 1.63 ppm, H_2O, reference to TSP,[11] 25 °C) is reversibly deprotonated to form the catalytically inactive[12] dinuclear hydroxo complex [(Cp*Ir^{III})$_2$(μ-OH)$_3$]$^+$ (**5**, Cp* at 1.61 ppm).[13] Similarly, ^{1}H NMR experiments show that, around pH 4.5, the catalyst precursor **2** (Cp* at 1.65 and 1.80 ppm) is reversibly deprotonated to form the catalytically inactive[12] dinuclear hydroxo complex [{(Cp∧py)Ir^{III}}$_2$(μ-OH)$_2$]$^{2+}$ (**6**, Cp* = 1.49 and 1.75 ppm). The structure of **6**$(OTf)_2$ was determined by X-ray analysis (Figure 3).[7,14] The Ir1···Ir2 distance (3.4266-(5) Å) in **6** is longer than that (3.071(1) Å) in **5**.[13] The two Cp* planes of **6** are arranged in an approximately parallel fashion (the torsion angle between the two least-squares planes is 1.2(5)°). Potentiometric titration experiments of the catalyst precursor **3** reveals that the practical pK_a value of **3** is 6.6. Alternatively, potentiometric titration of the catalytically inactive[12] mononuclear hydroxo complex [Cp*Ir^{III}(bpy)(OH)]$^+$ (**7**) also reveals one buffer region around pH 6.6. These results indicate that, around pH 6.6, complex **3** is reversibly deprotonated to form **7**. The structure of **7**(OTf)·$2H_2O$ was determined by X-ray analysis (Figure 4),[7,15] where all hydrogen atoms were included in the least-squares calculation of **7**. The Ir−O bond length (2.066(2) Å) in **7**(OTf) is shorter than that (2.154(2) Å) observed in **3**$(OTf)_2$.

Because of the difference in the electron-donating abilities of the Cp*, Cp∧py, and bpy ligands, the Lewis acidities of the iridium ions of **1**−**3** are ordered in strength as follows: **1** > **2** > **3**. The deprotonation behavior of **1**−**3** indicates that the more Lewis acidic iridium ions would lower the pK_a values of the coordinated H_2O ligands as shown in Scheme 1.

pH-Dependent Formation of the Active Catalysts. In the previous paper,[3a] we showed that, in the absence of the reducible substrates, the catalyst precursor **1** reacts with HCOONa to form the catalytically active dinuclear μ-hydride complex [(Cp*Ir^{III})$_2$(μ-H)(μ-OH)(μ-HCOO)]$^+$ (**8**). Figure 5a shows that complex **8** is

(9) Crystal data for **4**: $C_{15}H_{18}Cl_2IrN$, MW 475.44, triclinic, space group $P\bar{1}$ (No. 2) , a = 7.476(3) Å, b = 8.450(4) Å, c = 13.509(7) Å, α = 91.82(4)°, β = 98.14(4)°, γ = 112.87(3)°, V = 774.9(6) Å^3, Z = 2, D_c = 2.038 g cm^{-3}, μ(Mo Kα) = 89.69 cm^{-1}, R = 0.055, and R_w = 0.088.

(10) pD = pH meter reading + 0.4: Glasoe, P. K.; Long, F. A. *J. Phys. Chem.* **1960**, *64*, 188−190.

(11) TSP = 3-(trimethylsilyl)propionic-2,2,3,3-d_4 acid, sodium salt.

(12) The hydroxo complexes **5**−**7** are catalytically inactive for the reductions in this study.

(13) Nutton, A.; Bailey, P. M.; Maitlis, P. M. *J. Chem. Soc., Dalton Trans.* **1981**, 1997−2002.

(14) Crystal data for **6**$(OTf)_2$: $C_{30}H_{38}B_2F_8Ir_2N_2O_2$, MW 1016.69, triclinic, space group $P\bar{1}$ (No. 2) , a = 9.1972(5) Å, b = 11.202(2) Å, c = 16.973(2) Å, α = 80.779(5)°, β = 83.302(3)°, γ = 63.003(1)°, V = 1536.1(3) Å^3, Z = 2, D_c = 2.198 g cm^{-3}, μ(Mo Kα) = 87.60 cm^{-1}, R = 0.078, and R_w = 0.117.

(15) Crystal data for **7**(OTf)·$2H_2O$: $C_{21}H_{28}F_3IrN_2O_6S$, MW 685.74, monoclinic, space group $P2_1/c$ (No. 14), a = 11.222(2) Å, b = 13.379(1) Å, c = 16.4355(5) Å, β = 95.3476(8)°, V = 2456.9(5) Å^3, Z = 4, D_c = 1.854 g cm^{-3}, μ(Mo Kα) = 55.96 cm^{-1}, R = 0.037, and R_w = 0.056. The crystal structure of **7**(OTf)·$2H_2O$ reveals hydrogen bonds between the aqua ligand of **7** and the waters of crystallization.

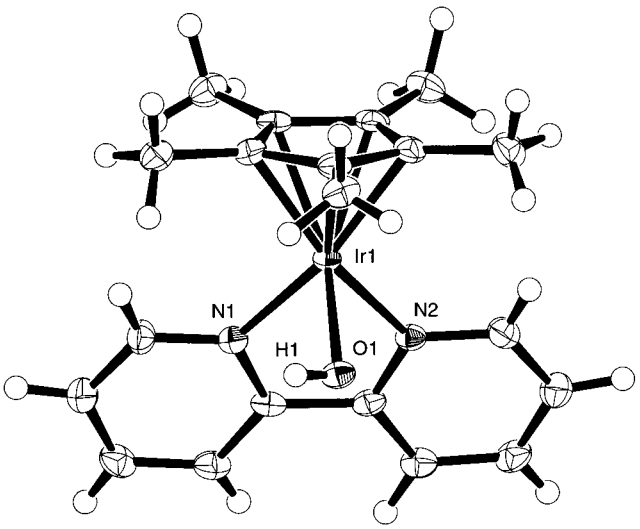

Figure 4. ORTEP drawing of **7**. The anion (OTf) is omitted for clarity. Selected bond lengths (Å) and angles (deg): Ir1−O1 = 2.066(2), Ir1−N1 = 2.098(4), Ir1−N2 = 2.084(4); O1−Ir1−N1 = 82.2(1), O1−Ir1−N2 = 80.3(1), N1−Ir1−N2 = 76.8(1).

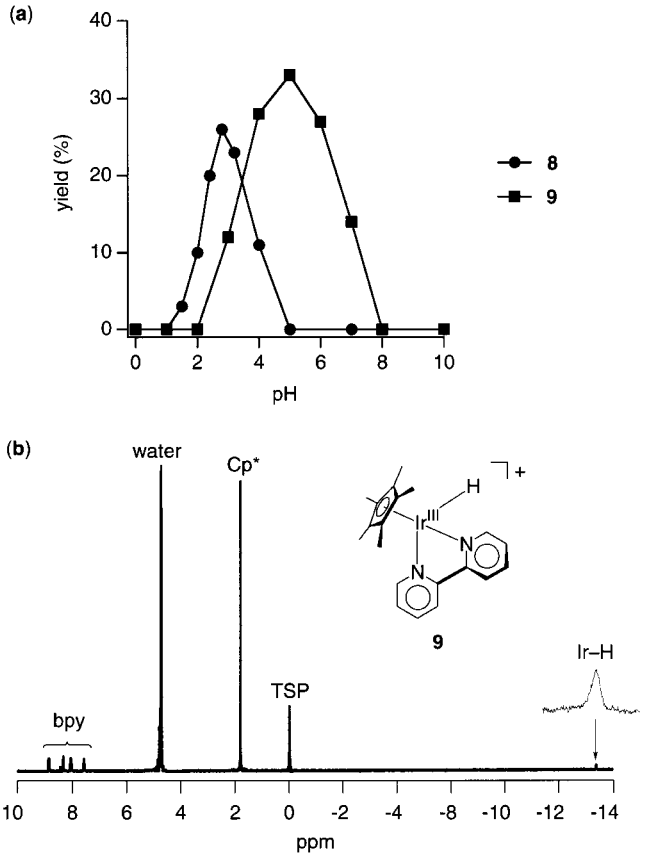

Figure 5. (a) pH-dependence profiles of the formation of **8** and **9** from the reaction of **1** and **3** with HCOONa. Conditions: complexes **1** and **3**, 10 μmol; HCOONa, 50 μmol; H_2O, 1 mL; pH 0.0−10.0; 1 h; 25 °C. (b) ^{1}H NMR spectrum (in D_2O at pH 5.0) of **9** which is in situ generated from the reaction of **3** with HCOONa.

generated at pH 2.8 (pD 3.2)[10] in the highest yield from the reaction of **1** with HCOONa. We propose a mechanism for the pH-dependent formation of **8** as follows. Above pH 2.8, HCOONa acts as $HCOO^-$ to bind the iridium atoms, because potentiometric titration experiments of HCOOH show that the pK_a value of HCOOH in the studied concentration is 2.8 (eq 1). Around pH

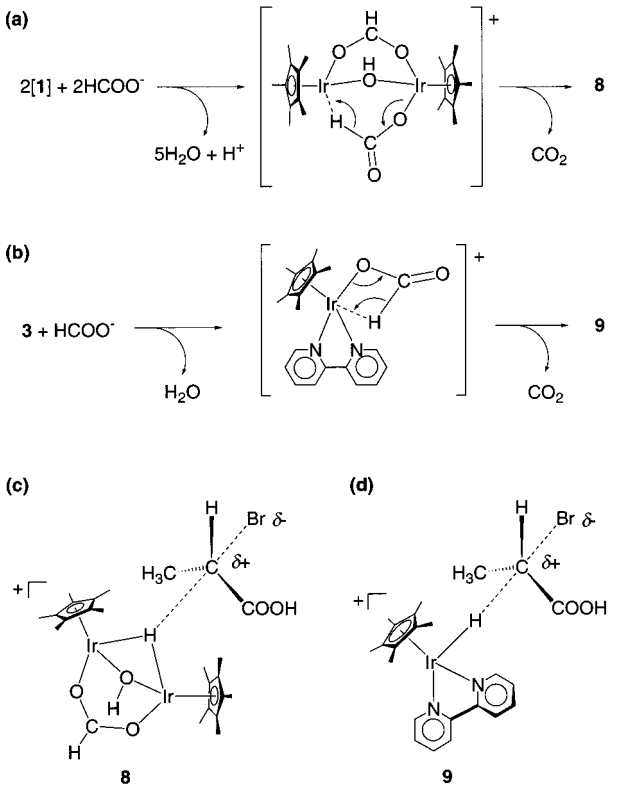

Figure 6. (a) Formation mechanism of **8** by β-hydrogen elimination with evolution of CO_2 in the reaction of **1** with $HCOO^-$. (b) Formation mechanism of **9** by β-hydrogen elimination with evolution of CO_2 in the reaction of **3** with $HCOO^-$. (c) Dehalogenation mechanism with **8**. (d) Dehalogenation mechanism with **9**.

$$HCOOH \overset{pK_a = 2.8}{\rightleftharpoons} HCOO^- + H^+ \qquad (1)$$

2.8, the catalyst precursor **1** is in equilibrium with the catalytically inactive **5**. Thus, around pH 2.8, the addition of HCOONa to the equilibrium mixture provides **8** through a β-hydrogen elimination with evolution of CO_2 (Figure 6a). We here disclose the crystal structure of **8**(PF_6) by X-ray analysis (Figure 7).[7,16] The Ir1···Ir2 distance is 2.7781(7) Å. The torsion angle between the two least-squares planes of Cp* of **8**(PF_6) is 62.5(8)°.

In a pH range of about 3−5, in the absence of the reducible substrates, the catalyst precursor **2** reacts with the formate ions to evolve CO_2. The evolution of CO_2 has been confirmed by GC analysis.[17] At this stage, however, we have no definite structural information on the hydride species to be formed from the reaction of **2** with the formate ions.

In a pH range of about 2−8, in the absence of the reducible substrates, the catalyst precursor **3** reacts with the formate ions to form the hydride complex $[Cp^*Ir^{III}(bpy)(H)]^+$ (**9**) through a β-hydrogen elimination with evolution of CO_2 (Figure 6b). The evolution of CO_2

(16) Crystal data for **8**(PF_6): $C_{21}H_{33}F_6Ir_2O_3P$, MW 862.89, orthorhombic, space group $P2_12_12_1$ (No. 19), a = 11.655(2) Å, b = 13.5242(5) Å, c = 16.5798(5) Å, V = 2613.3(4) Å^3, Z = 4, D_c = 2.193 g cm^{-3}, μ(Mo Kα) = 103.26 cm^{-1}, R = 0.068, and R_w = 0.092.

(17) Shimadzu gas chromatograph, GC-8A with Unibeads C.

Downloaded by CARLI CONSORTIUM on June 29, 2009
Published on September 27, 2001 on http://pubs.acs.org | doi: 10.1021/om010523v

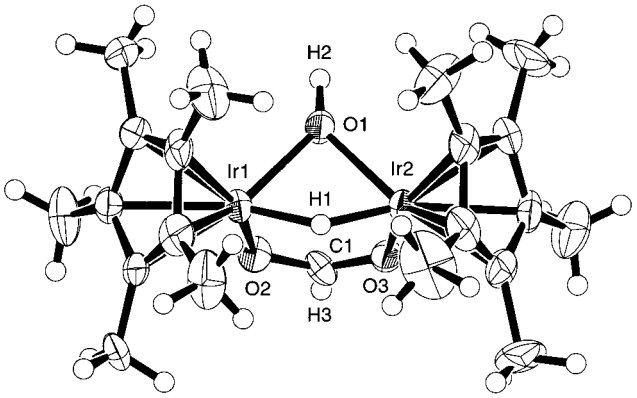

Figure 7. ORTEP drawing of **8**. The anion (PF_6) is omitted for clarity. Selected bond lengths (Å) and angles (deg): Ir1−H1 = 1.53, Ir2−H1 = 1.51, Ir1−O1 = 2.10(1), Ir1−O2 = 2.10(1), Ir2−O1 = 2.101(10), Ir2−O3 = 2.114(10), O2−C1 = 1.26(2), O3−C1 = 1.25(2); Ir1−O1−Ir2 = 82.9(3), Ir1−O2−C1 = 124.7(9), Ir2−O3−C1 = 124.7(9), O2−C1−O3 = 125(1).

has also been confirmed by GC analysis.[17] Steckhan et al. have proposed the formation of $[Cp^*Rh^{III}(bpy)(H)]^+$ from the reaction of $[Cp^*Rh^{III}(bpy)(H_2O)]^{2+}$ with HCOONa through the same β-hydrogen elimination.[18] Figure 5a shows that complex **9** is in situ generated at pH 5.0 in the highest yield from the reaction of **3** with HCOONa. As shown in Figure 5b, the ^1H NMR spectrum (D_2O, reference to TSP,[11] 25 °C, pH 5.0) of **9** provides H^- (−11.3 ppm), Cp* (1.83 ppm), and bpy (7.6, 8.1, 8.3, and 8.9 ppm) signals.

Conditions of the pH-Dependent Reductions. The pH-dependent transfer hydrogenation, reductive amination, and dehalogenation of water-soluble substrates (10 μmol) with **1**−**3** as catalyst precursors (1 μmol) and HCOONa and $HCOONH_4$ as hydrogen donors (10−50 μmol) in water (1 mL) were investigated at 25 °C. It has been confirmed that the catalytic reductions do not occur in the absence of **1**−**3** (as blank experiments). In the course of the reaction, the pH of the solution was monitored, and it was confirmed that the pH of the solution does not change during the course of the reactions under the conditions of this study. The solution was stirred at 25 °C under an Ar atmosphere. Products were determined by ^1H NMR (internal standard: TSP[11]). Initial turnover frequencies (TOF) are expressed as the number of moles of product formed per mole of catalyst after 1 h of the reaction.

pH-Dependent Transfer Hydrogenation. The series of carbonyl compounds examined in this study are an aldehyde (*n*-butyraldehyde (**a**), Table 1), a ketone (2-butanone (**b**)), an aldehyde acid (glyoxylic acid (**c**)), and a keto acid (pyruvic acid (**d**)). Interestingly, although the transfer hydrogenation of the carbonyl compounds with **1** proceeds, the transfer hydrogenation with **3** does not occur under the conditions of this study. We propose that the dinuclear active catalyst **8** has a potentially vacant site for the incoming substrate (because the total electrons for **8** is 34), but the mononuclear active catalyst **9** does not have the vacant site for the incoming substrate. In the transfer hydrogenation with **1** and **2**, the rate of reduction of the aldehyde (**a**) is faster than that of the ketone (**b**). Thus, the reduction of the aldehyde group in **c** takes place easily, while the reduction of the ketone group of **d** does not occur. Figure 8a shows pH-dependent profiles of the transfer hydrogenation of **a** with **1**−**3**, indicating that the rate of the transfer hydrogenation promoted by **1** and **2** shows sharp maximums at pH 2.8 and 3.5, respectively. Figure 8b shows the time course of turnover numbers (TON) of these transfer hydrogenations. In addition, the rate of this transfer hydrogenation is dependent on the concentration of HCOONa.

pH-Dependent Reductive Amination. By utilizing $HCOONH_4$ (eq 2) as a hydrogen donor ($HCOO^-$) as well as an amine donor (NH_4^+), we have investigated the pH-dependent reductive amination of **a**−**d** with **1**, **2**, and **3** at 25 °C (Table 1). It is important to note that the pK_a value of NH_4^+ is 4.7 (eq 3). Thus, above pH 4.7, the

$$HCOONH_4 \rightleftharpoons HCOO^- + NH_4^+ \quad (2)$$

$$NH_4^+ \overset{pK_a = 4.7}{\rightleftharpoons} NH_3 + H^+ \quad (3)$$

$$>C{=}O + NH_3 \overset{-OH^-}{\rightleftharpoons} \left[>C{=}\overset{\oplus}{N}\begin{matrix}H\\H\end{matrix}\right] \overset{-H^+}{\rightleftharpoons} >C{=}N\!:\!H \quad (4)$$

iminium ion imine

aldehydes and ketones react with NH_3 to provide the corresponding iminium ions[19] or imines (eq 4), which can be reduced by iridium hydrides. Figure 9a shows pH-dependent profiles of the reductive amination of **a** with **1**−**3**, indicating that the rate of the reductive amination with **1**−**3** shows maximums at pH 2.8, 3.5, and 5.0, respectively. The reductive amination of **a** with **3** proceeds much more efficiently than that with **2** or **1.** Figure 9b shows the time course of TON of these reductive aminations. The rate of this reductive amination is also dependent on the concentration of $HCOONH_4$. In addition, the reductive amination of **b**−**d** was not observed under these conditions.

pH-Dependent Dehalogenation. We have examined the dehalogenation of three water-soluble alkyl halides: 2-bromopropanoic acid (**e**), 2-chloropropanoic acid (**f**), and 3-bromopropanoic acid (**g**) at 25 °C. Intriguingly, Table 1 shows that the dehalogenation of the alkyl halides with **1** does not occur. If dehalogenation is an S_N2 type reaction, then the active catalyst **8** (Figure 6c) is too bulky to make the S_N2 intermediate compared with **9** (Figure 6d). Therefore, the rates of the dehalogenation of **f** and **g** with **3** and HCOONa at pH 5.0 could be much slower than that of **e** (Table 1). Figure 10a shows pH-dependent profiles of the dehalogenation of **e** with **1**−**3**. It has been confirmed by ^1H NMR that the labeled hydrogen atom is incorporated into **e** when DCOONa is used as the hydrogen donor in the dehalogenation with **3** (eq 5). The rate of the dehalogenation

$$H_3C{-}\overset{H}{\underset{Br}{C}}{-}COOH + DCOONa \xrightarrow[pH\ 5.0]{3} H_3C{-}\overset{H}{\underset{D}{C}}{-}COOH + CO_2 + Na^+ + Br^- \quad (5)$$

of **e** with **2** and **3** shows maximums at pH 3.5 and 5.0, respectively. Figure 10b shows the time course of TON of these dehydrogenations, indicating that, after 4 h, the

(18) Hollmann, F.; Schmid, A.; Steckhan, E. *Angew. Chem., Int. Ed.* **2001**, *40*, 169−171.

(19) Iminium ions are reduced much faster than carbonyl compounds by $NaBH_3CN$ at pH 6−8: Lane, C. F. *Synthesis* **1975**, 135−146.

Downloaded by CARLI CONSORTIUM on June 29, 2009
Published on September 27, 2001 on http://pubs.acs.org | doi: 10.1021/om010523v

Table 1. Transfer Hydrogenation, Reductive Amination, and Dehalogenation of Water-Soluble Substrates with Catalyst Precursors (1−3) and Hydrogen Donors (HCOONa and $HCOONH_4$)[a]

substrates		hydrogen donors	products	initial TOF[b] with **1** at pH 2.8	with **2** at pH 3.5	with **3** at pH 5.0
$HC(=O)-CH_2CH_2CH_3$	(**a**)	HCOONa	$H_2C(OH)-CH_2CH_2CH_3$	1.5	0.5	0.0
$H_3C-C(=O)-CH_2CH_3$	(**b**)	HCOONa	$H_3C-CH(OH)-CH_2CH_3$	0.5	0.1	0.0
$HC(=O)-COOH$	(**c**)	HCOONa	$H_2C(OH)-COOH$	4.3	1.8	0.0
$H_3C-C(=O)-COOH$	(**d**)	HCOONa	$H_3C-CH(OH)-COOH$	0.0	0.0	0.0
$HC(=O)-CH_2CH_2CH_3$	(**a**)	$HCOONH_4$	$H_2C(NH_2)-CH_2CH_2CH_3$	0.1	0.2	2.1
			$H_2C(OH)-CH_2CH_2CH_3$	1.0	0.2	0.0
$H_3C-C(=O)-CH_2CH_3$	(**b**)	$HCOONH_4$	$H_3C-CH(NH_2)-CH_2CH_3$	0.0	0.0	0.0
			$H_3C-CH(OH)-CH_2CH_3$	0.5	0.1	0.0
$HC(=O)-COOH$	(**c**)	$HCOONH_4$	$H_2C(NH_2)-COOH$	0.0	0.0	0.0
			$H_2C(OH)-COOH$	4.2	1.7	0.0
$H_3C-C(=O)-COOH$	(**d**)	$HCOONH_4$	$H_3C-CH(NH_2)-COOH$	0.0	0.0	0.0
			$H_3C-CH(OH)-COOH$	0.0	0.0	0.0
$H_3C-C(H)(Br)-COOH$	(**e**)	HCOONa	CH_3CH_2COOH	0.0	0.8	6.3
$H_3C-C(H)(Cl)-COOH$	(**f**)	HCOONa	CH_3CH_2COOH	0.0	0.0	0.1
$H_2C(Br)-CH_2COOH$	(**g**)	HCOONa	CH_3CH_2COOH	0.0	0.0	0.2

[a] Conditions: **1**, **2**, or **3**, 1 μmol; substrates, 10 μmol; HCOONa and $HCOONH_4$, 50 μmol; H_2O, 1 mL; 25 °C. [b] The initial TOF is equal to (mol of products)/(mol of **1**, **2**, or **3**) after 1 h of the reaction.

Downloaded by CARLI CONSORTIUM on June 29, 2009
Published on September 27, 2001 on http://pubs.acs.org | doi: 10.1021/om010523v

reduction of **e** with **3** is almost completed. In addition, the rate of this dehalogenation is dependent on the concentration of HCOONa.

Conclusions

We have demonstrated the potential of the organometallic aqua complexes **1**−**3** to be pH-dependent catalyst precursors for transfer hydrogenation, reductive amination, and dehalogenation of water-soluble carbonyl compounds and alkyl halides with HCOONa and $HCOONH_4$ as hydrogen donors in water at ambient temperature. The trends of these reactions are summarized in Figure 11. Each catalyst shows different selectivity for three reactions. The selectivity could be governed by the following factors: (i) the deprotonation behavior of the H_2O ligands in the catalyst precursors, (ii) the pH-dependent behavior of the hydrogen donors HCOONa (pK_a of HCOOH 2.8) and $HCOONH_4$ (pK_a of NH_4^+ 4.7), (iii) the pH-dependent formation of the active catalysts, and (iv) the structural features (e.g. a possible vacant site for the incoming substrate and bulkiness) of the active catalysts.

Experimental Section

Materials and Methods. All experiments were carried out under an Ar atmosphere at ambient temperature. All chemicals (highest purity available) were purchased from Aldrich Chemicals Co. and used without further purification. The ^1H and ^{13}C NMR spectra were recorded on an JEOL JNM-EX 270 spectrometer. The potentiometric titration experiments were performed on a TOA pH meter Model HM-18E) with a TOA pH combination electrode (Model GS-5015C).

pH Adjustment. The pH of the solution was adjusted by using 1 M $HClO_4/H_2O$ (1 M $DClO_4/D_2O$) and 0.1 M $NaOH/H_2O$ (0.1 M $NaOD/D_2O$). In the pH range 2−10, the pH of the solution was determined by a pH meter, but below pH 1, it was assumed by the concentration of the solution, e.g., pH values of 0.1 and 1 M $HClO_4/H_2O$ were assumed to be 1 and 0, respectively. Buffer was not used to control pH, since the pH of the solution did not change during the course of the reactions under the conditions of this study. To determine the exact pH values of the ^1H NMR samples, the ^1H NMR experiments were performed by dissolving the samples in H_2O in an NMR tube (diameter 5.0 mm) with a sealed capillary tube (diameter 1.5 mm) containing TSP[11] (100 mM) dissolved in D_2O (for deuterium lock).

Downloaded by CARLI CONSORTIUM on June 29, 2009
Published on September 27, 2001 on http://pubs.acs.org | doi: 10.1021/om010523v

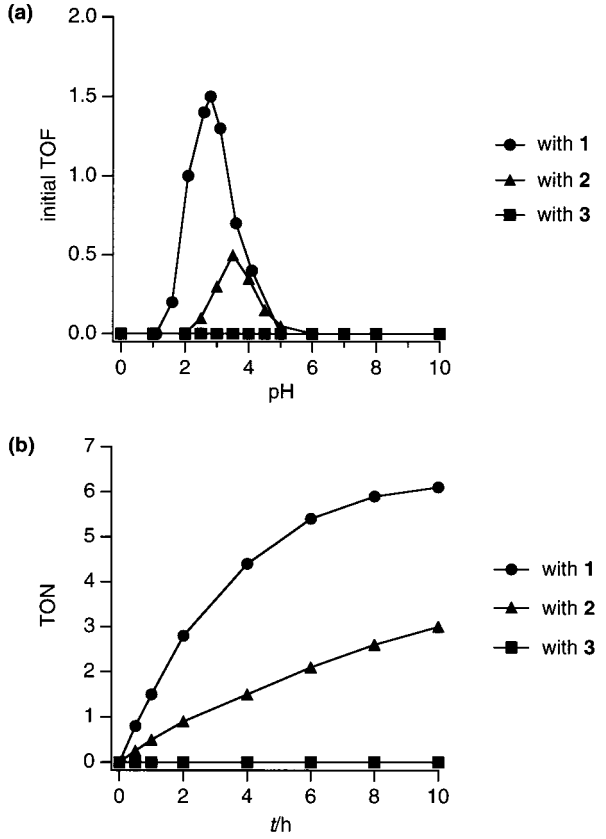

Figure 8. (a) Typical pH-dependence profile of the transfer hydrogenation of *n*-butyraldehyde (**a**) with **1**, **2**, or **3** (the initial TOF is equal to (mol of products)/(mol of **1**, **2**, or **3**) after 1 h of the reaction). (b) Time course of turnover numbers (TON) of the transfer hydrogenation of *n*-butyraldehyde (**a**) with **1** (at pH 2.8), **2** (at pH 3.5), or **3** (at pH 5.0). Conditions: complex **1**, **2**, or **3**, 1 μmol; *n*-butyraldehyde, 10 μmol; HCOONa, 50 μmol; H_2O, 1 mL; 25 °C.

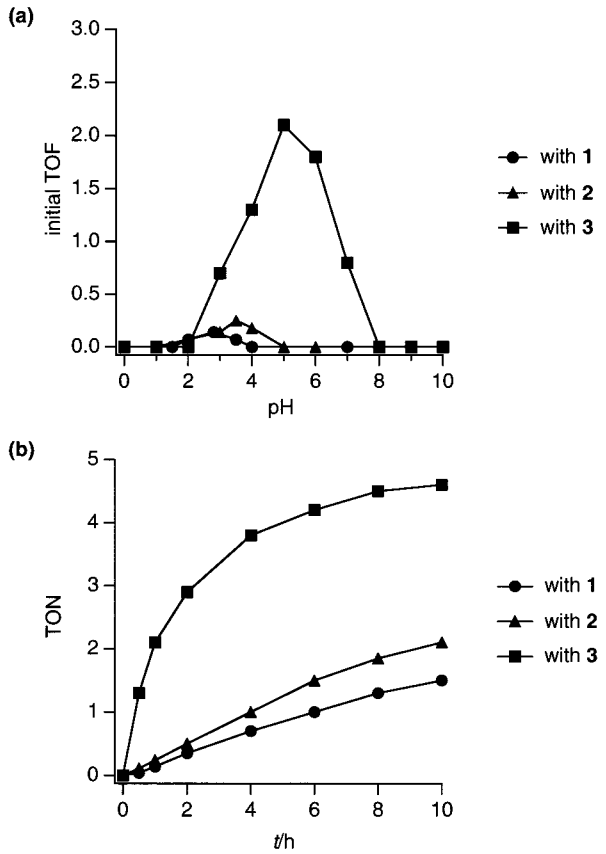

Figure 9. (a) Typical pH-dependence profile of the reductive amination of *n*-butyraldehyde (**a**) with **1**, **2**, or **3** (the initial TOF is equal to (mol of products)/(mol of **1**, **2**, or **3**) after 1 h of the reaction). (b) Time course of TON of the reductive amination of *n*-butyraldehyde (**a**) with **1** (at pH 2.8), **2** (at pH 3.5), or **3** (at pH 5.0). Conditions: complex **1**, **2**, or **3**, 1 μmol; *n*-butyraldehyde, 10 μmol; $HCOONH_4$, 50 μmol; H_2O, 1 mL; 25 °C.

H(Cp∧py). Into a 200 mL flask were charged diisopropylamine (3.5 mL, 25 mmol) and THF (50 mL), and then ^{n}BuLi (15.6 mL, 25 mmol, 1.6 M in hexane) was added dropwise with stirring at 0 °C. The resulting solution was warmed to ambient temperature and stirred for another 30 min. The solution was cooled to −20 °C, and 2-picoline (2.3 g, 25 mmol) was added dropwise over 20 min. The resulting solution was warmed to ambient temperature and stirred for another 1 h. The solution was cooled to −20 °C, and 2,3,4,5-tetramethyl-2-cyclopentenone (3.8 mL, 25 mmol) was added dropwise over 10 min. The resulting solution was warmed to ambient temperature and stirred overnight. The reaction mixture was quenched with 50 mL of saturated solution of $NaHCO_3$, and the organic layer was extracted with 150 mL of ether. The extract was dried over anhydrous K_2CO_3, filtered, and concentrated to yield an oil. Into a 300 mL flask were charged the oil and ether (100 mL), and *p*-toluenesulfonic acid monohydrate (5 g, 26 mmol) was added over 3 min. After it was stirred overnight at ambient temperature, the reaction mixture was quenched with 100 mL of a saturated solution of potassium carbonate. The pH of the solution was adjusted to about 10 by the addition of K_2CO_3. The organic layer was extracted with 150 mL of ether. The extract was dried over anhydrous K_2CO_3, filtered, and concentrated to yield an oil of crude H(Cp∧py). The crude H(Cp∧py) was purified by alumina column chromatography (Merck, Aluminiumoxid 60 1067) with ethyl acetate and hexane (2:98) as eluent to isolate a colorless oil of H(Cp∧py) (yield 60% based on 2-picoline). ^{1}H NMR ($CDCl_3$, reference to TMS, 25 °C): δ 1.01 (d, 3H, CH_3), 1.08 (d, 3H, CH_3), 1.63 (s, 3H, CH_3), 1.81 (m, 9H, CH_3), 1.89 (m, 6H, CH_3), 2.5−2.7 (m, 2H, CH), 3.69 (d, 1H, CH_2), 3.81 (s, 2H, CH_2), 3.92 (d, 1H, CH_2), 6.96 (d, 1H, py), 7.06 (m, 3H, py), 7.53 (m, 2H, py), 8.51 (m, 2H, py). Anal. Calcd for H(Cp∧py): $C_{15}H_{19}N$: C, 84.46; H, 8.98; N, 6.57. Found: C, 84.44; H, 9.20; N, 6.36.

$[(Cp\wedge py)Ir^{III}(H_2O)_2]^{2+}$ (2). A solution of **4** (1.43 g, 3.00 mmol) and $AgBF_4$ (1.17 g, 6.00 mmol) in H_2O (20 mL, pH of the solution ca. 3.0) was stirred at ambient temperature for 12 h under Ar, and the precipitating AgCl was removed by filtration. The solvent was evaporated to yield a yellow powder of **2**$(BF_4)_2$, which was dried in vacuo (yield 98% based on **4**). ^{1}H NMR (D_2O, reference to TSP, pH 3.0, 25 °C): δ 1.65 (s, 6H, η^5-$C_5(CH_3)_4$), 1.80 (s, 6H, η^5-$C_5(CH_3)_4$), 4.13 (s, 2H, methylene), 7.59 (m, 2H, py), 8.00 (d, J = 5.6 Hz, 1H, py), 8.10 (t, J = 7.9 Hz, 1H, py). ^{13}C NMR (D_2O, reference to TSP, pH 3.0, 25 °C): δ 10.8 (s, η^5-$C_5(CH_3)_4$), 11.5 (s, η^5-$C_5(CH_3)_4$), 34.7 (s, methylene), 77.5 (s, η^5-$C_5(CH_3)_4$), 96.6 (s, η^5-$C_5(CH_3)_4$), 97.2 (s, η^5-$C_5(CH_3)_4$), 128.1 (s, py), 128.6 (s, py), 143.9 (s, py), 150.9 (s, py), 178.4 (s, py). Anal. Calcd for **2**$(BF_4)_2\cdot H_2O$: $C_{15}H_{24}B_2F_8IrNO_3$: C, 28.50; H, 3.83; N, 2.22. Found: C, 28.80; H, 3.72; N, 2.22.

$[Cp^*Ir^{III}(bpy)(H_2O)]^{2+}$ (3). A solution of **1**$(OTf)_2$ (2.04 g, 3.0 mmol) and bpy (469 mg, 3.0 mmol) in H_2O (20 mL, pH of the solution ca. 3.0) was stirred at ambient temperature for 6 h under Ar. The solvent was evaporated to yield a yellow powder of **3**$(OTf)_2$, which was dried in vacuo (yield 99% based on **1**$(OTf)_2$). ^{1}H NMR (D_2O, reference to TSP, pH 3.0, 25 °C): δ 1.69 (s, 15H, η^5-$C_5(CH_3)_5$), 7.91 (t, J = 5.6 Hz, 2H, H-5,5′), 8.36 (t, J = 7.9 Hz, 2H, H-4,4′), 8.57 (d, J = 7.9 Hz, 2H, H-3,3′), 9.14 (d, J = 5.6 Hz, 2H, H-6,6′). ^{13}C NMR (D_2O, reference to TSP, pH 3.0, 25 °C): δ 10.6 (s, η^5-$C_5(CH_3)_5$), 92.2 (s, η^5-$C_5(CH_3)_5$), 127.2 (s, C-3,3′), 132.1 (s, C-5,5′), 144.5 (s, C-4,4′), 154.4

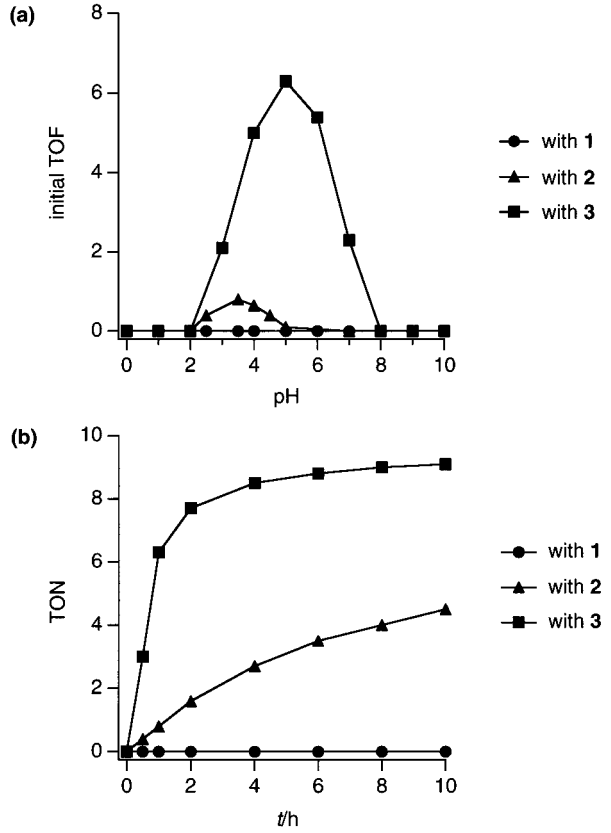

Figure 10. (a) Typical pH-dependence profile of the dehalogenation of 2-bromopropanoic acid (**e**) with **1**, **2**, or **3**. (the initial TOF is equal to (mol of products)/(mol of **1**, **2**, or **3**) after 1 h of the reaction). (b) Time course of TON of the dehalogenation of 2-bromopropanoic acid (**e**) with **1** (at pH 2.8), **2** (at pH 3.5), or **3** (at pH 5.0). Conditions: complex **1**, **2**, or **3**, 1 μmol; 2-bromopropanoic acid, 10 μmol; HCOONa, 50 μmol; H_2O, 1 mL; 25 °C.

(s, C-6,6′), 158.9 (s, C-2,2′). Anal. Calcd for **3**$(OTf)_2 \cdot H_2O$: $C_{22}H_{27}F_6IrN_2O_8S_2$: C, 32.31; H, 3.33; N, 3.43. Found: C, 32.54; H, 3.21; N, 3.56.

[(Cp∧py)Ir^{III}Cl$_2$] (4). In a 500 mL flask were placed $IrCl_3 \cdot 3H_2O$ (4.6 g, 13.1 mmol), molecular sieve 4A (80 g), 1,2-dichloroethane (200 mL), and ethanol (20 mL). The solution was stirred at ambient temperature for 30 min, and then H(Cp∧py) was added (2.8 g, 13.1 mmol). The reaction solution was stirred at reflux temperature for 48 h. The reaction solution was filtered, and the solvent was removed under reduced pressure to yield crude **4**. The crude product was purified by silica gel column chromatography (Wakogel C-200E) with dichloromethane and methanol (99:1) as eluent to yield brown solids of **4** (yield 35% based on $IrCl_3 \cdot 3H_2O$). ^{1}H NMR ($CDCl_3$, reference to TMS, 25 °C): δ 1.79 (s, 6H, η^5-$C_5(CH_3)_4$), 1.85 (s, 6H, η^5-$C_5(CH_3)_4$), 3.84 (s, 2H, methylene), 7.20 (d, J = 7.9 Hz, 1H, py), 7.33 (t, J = 7.3 Hz, 1H, py), 7.77 (t, J = 7.9 Hz, 1H, py), 8.62 (d, J = 7.3 Hz, 1H, py). ^{13}C NMR ($CDCl_3$, reference to TMS, 25 °C): δ 8.52 (s, η^5-$C_5(CH_3)_4$), 9.2 (s, η^5-$C_5(CH_3)_4$), 32.7 (s, methylene), 90.28 (s, η^5-$C_5(CH_3)_4$), 92.2 (s, η^5-$C_5(CH_3)_4$), 122.4 (s, py), 125.2, (s, py), 138.4 (s, py), 152.6 (s, py), 175.3 (s, py). Anal. Calcd for **4**: $C_{15}H_{18}IrNCl_2$: C, 37.89; H, 3.82; N, 2.95. Found: C, 37.67; H, 3.86; N, 2.90.

X-ray Crystallographic Analysis. Yellow crystals of **3**$(OTf)_2 \cdot H_2O$ used in X-ray structure analysis were obtained from an aqueous solution of **3**$(OTf)_2$ at pH 3.0. Orange crystals of **4** were obtained by diffusion of diethyl ether into a methanol solution of **4** at ambient temperature. Yellow crystals of **6**$(OTf)_2$ were obtained from an aqueous solution of **2**$(OTf)_2$ at pH 7.0. Yellow crystals of **7**$(OTf) \cdot 2H_2O$ were obtained from an aqueous solution of **3**$(OTf)_2$ at pH 10.0. Orange crystals of **8**(PF_6) were obtained by diffusion of diethyl ether into a methanol solution of **8**(PF_6) at ambient temperature. Measurements were made on a Rigaku/MSC Mercury CCD diffractometer (for **3**$(OTf)_2 \cdot H_2O$, **6**$(OTf)_2$, **7**$(OTf) \cdot 2H_2O$, and **8**(PF_6)) and a Rigaku AFC7R four-circle diffractometer (for **4**) with graphite-monochromated Mo Kα radiation (λ = 0.7107 Å). All calculations were performed using the teXsan crystallographic software package of Molecular Structure Corp. Crystal data, data collection parameters, structure solution and refinement details, atomic coordinates, anisotropic displacement parameters, bond lengths, and bond angles are given in the Supporting Information.

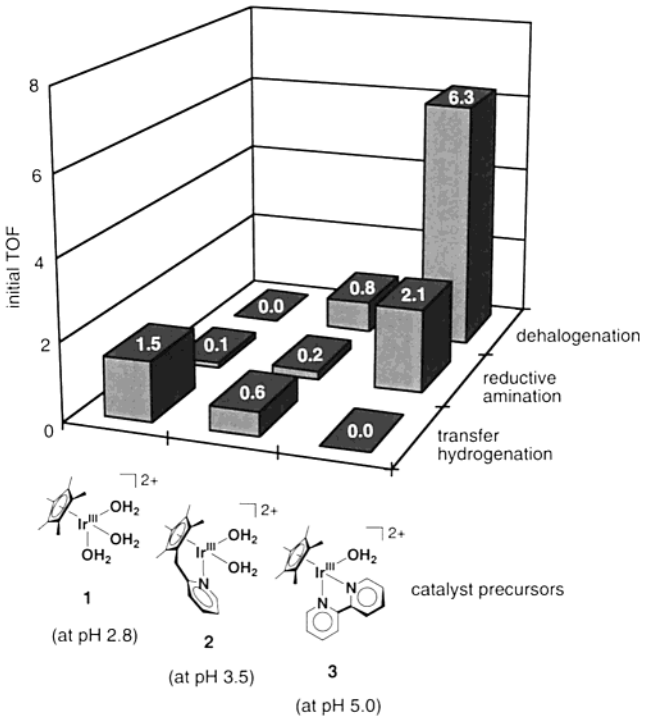

Figure 11. Catalytic reductions of the water-soluble substrates with the aqua complexes **1**−**3** and the formate ions (the initial TOF is equal to (mol of products)/(mol of **1**, **2**, or **3**) after 1 h of the reaction). Conditions: complex **1**, **2**, or **3**, 1 μmol; substrates, 10 μmol (*n*-butyraldehyde for transfer hydrogenation, *n*-butyraldehyde for reductive amination, 2-bromopropanoic acid for dehalogenation); HCOONa (or $HCOONH_4$), 50 μmol; H_2O, 1 mL; 25 °C.

Acknowledgment. Financial support of this research by the Ministry of Education, Science, Sports, and Culture, Japan Society for the Promotion of Science, Grant-in-Aid for Scientific Research, to S.O. (Grant No. 13640568) and Y.W. (Grant Nos. 11490036 and 11228208) is gratefully acknowledged. We thank Professor K. Isobe (Osaka City University) for valuable discussions.

Supporting Information Available: Crystallographic information for **3**$(OTf)_2 \cdot H_2O$, **6**$(OTf)_2$, **7**$(OTf) \cdot 2H_2O$, and **8**(PF_6). This material is available free of charge via the Internet at http://pubs.acs.org.

OM010523V

Downloaded by CARLI CONSORTIUM on June 29, 2009
Published on September 27, 2001 on http://pubs.acs.org | doi: 10.1021/om010523v